1 # BED-domain containing immune receptors confer

2 # diverse resistance spectra to yellow rust

3

4 Clemence Marchal[1*], Jianping Zhang[2,3*], Peng Zhang[4], Paul Fenwick[5], Burkhard

5 Steuernagel[1], Nikolai M. Adamski[1], Lesley Boyd[6], Robert McIntosh[4], Brande B.H. Wulff[1],

6 Simon Berry[5], Evans Lagudah[2], Cristobal Uauy[1†]

7

8

9 [1] John Innes Centre, Norwich Research Park, Norwich NR4 7UH, United Kingdom

10 [2] Commonwealth Scientific and Industrial Research Organization (CSIRO) Agriculture &

11 Food, Canberra, ACT 2601, Australia

12 [3] Henan Tianmin Seed Company Limited, Lankao County, 475300, Henan Province, China

13 [4] University of Sydney, Plant Breeding Institute, Cobbitty, NSW 2570, Australia

14 [5] Limagrain UK Ltd, Rothwell, Market Rasen, Lincolnshire, LN7 6DT, United Kingdom

15 [6] NIAB, Huntingdon Road, Cambridge, CB3 0LE, United Kingdom

16

17 *Clemence Marchal and Jianping Zhang contributed equally to this work

18 [†] Correspondence to cristobal.uauy@jic.ac.uk

19 **Introductory paragraph**

20   Crop diseases reduce wheat yields by ~25% globally and thus pose a major threat to global

21   food security[1]. Genetic resistance can reduce crop losses in the field and can be selected for

22   through the use of molecular markers. However, genetic resistance often breaks down

23   following changes in pathogen virulence, as experienced with the wheat yellow (stripe) rust

24   fungus *Puccinia striiformis* f. sp. *tritici* (*Pst*)[2]. This highlights the need to (i) identify genes

25   that alone or in combination provide broad-spectrum resistance and (ii) increase our

26   understanding of the underlying molecular modes of action. Here we report the isolation and

27   characterisation of three major yellow rust resistance genes (*Yr7*, *Yr5*, and *YrSP*) from

28   hexaploid wheat (*Triticum aestivum*), each having a distinct and unique recognition

29   specificity. We show that *Yr5*, which remains effective to a broad range of *Pst* isolates

30   worldwide, is allelic to *YrSP* and paralogous to *Yr7*, both of which have been overcome by

31   multiple *Pst* isolates. All three *Yr* genes belong to a complex resistance gene cluster on

32   chromosome 2B encoding nucleotide-binding and leucine-rich repeat proteins (NLRs) with a

33   non-canonical N-terminal zinc-finger BED domain[3] that is distinct from those found in non-

34   NLR wheat proteins. We developed diagnostic markers to accelerate haplotype analysis and

35   for marker-assisted selection to enable the stacking of the non-allelic *Yr* genes. Our results

36   provide evidence that the BED-NLR gene architecture can provide effective field-based

37   resistance to important fungal diseases such as wheat yellow rust.

38

39   **Main**

40   In plant immunity, NLRs act as intracellular immune receptors that upon pathogen

41   recognition trigger a series of signalling steps that ultimately lead to cell death, thus

42   preventing the spread of infection[4,5]. The NB-ARC domain is the hallmark of NLRs which in

43   most cases include leucine-rich repeats (LRRs) at the C-terminus. Recent *in silico* analyses

44   have identified NLRs with additional 'integrated' domains[6–8], including zinc-finger BED

45   domains (BED-NLRs). The BED domain function within BED-NLRs is unknown, although

46   the BED domain from the non-NLR DAYSLEEPER protein was shown to bind DNA in

47   *Arabidopsis*[9]. BED-NLRs are widespread across Angiosperm genomes[6–8] and this gene

48   architecture has been shown to confer resistance to bacterial blast in rice (*Xa1*[10,11]).

49

50   The genetic relationship between *Yr5* and *Yr7* has been debated for almost 45 years[12,13]. Both

51   genes map to chromosome arm 2BL in hexaploid wheat and were hypothesized to be

52   allelic[14], and closely linked with *YrSP*[15]. Whilst only one of >6,000 tested *Pst* isolates

53   worldwide has been found virulent to *Yr5* (Supplementary Table 1[14,16]), both *Yr7* and *YrSP*

54   have been overcome in the field. For *Yr7*, this is likely due to its wide deployment in cultivars

55   (Supplementary Table 2, Supplementary Figure 1). This highlights the importance of

56   stewardship plans (including diagnostic markers) to deploy *Yr5* in combination with other

57   genes as currently done in the US (e.g. *Yr5*+*Yr15*; UC Davis breeding programme).

58

59   To clone the genes encoding *Yr7, Yr5,* and *YrSP*, we identified susceptible ethyl

60   methanesulfonate-derived (EMS) mutants from different genetic backgrounds carrying these

61   genes (Figure 1, Supplementary Tables 3-4). We performed MutRenSeq[17] and isolated a

62   single candidate contig for each of the three genes based on nine, ten, and four independent

63   susceptible mutants, respectively (Figure 1a; Supplementary Figure 2). The three candidate

64   contigs were genetically linked to a common mapping interval, previously identified for the

65   three *Yr* loci[15,18,19]. Their closest homologs in the Chinese Spring wheat genome sequence

66   (RefSeq v1.0) all lie within this common genetic interval (Figure 1b; Supplementary Figure

67   3).

68

3

69   Within each contig we predicted a single open reading frame based on RNA-Seq data. All

70   three predicted *Yr* genes displayed similar exon-intron structures (Figure 1a), although *YrSP*

71   was truncated in exon 3 due to a single base deletion that resulted in a premature termination

72   codon. The DNA sequences of *Yr7* and *Yr5* were 77.9% identical across the complete gene;

73   whereas *YrSP* was a truncated version of *Yr5*, sharing 99.8% identity in the common

74   sequence (Supplementary Files 1 and 2). This suggests that *Yr5* and *YrSP* are encoded by

75   alleles of the same gene, but are paralogous to *Yr7*. The 23 mutations identified by

76   MutRenSeq were confirmed by Sanger sequencing and all lead to either an amino acid

77   substitution or a truncation allele (splice junction or termination codon) (Figure 1a;

78   Supplementary Table 4). Taken together, the mutant and genetic analyses demonstrate that

79   *Yr5* and *YrSP* are allelic, while *Yr7* is encoded by a related, yet distinct gene.

80

81   The Yr7, Yr5, and YrSP proteins contain a zinc-finger BED domain at the N-terminus,

82   followed by the canonical NB-ARC domain. Unlike previously cloned resistance genes in

83   grasses (e.g. *Mla10l*[20], *Sr33*[21], *Pm3*[22]), neither *Yr7* nor *Yr5*/*YrSP* encode Coiled Coil domains

84   at the N-terminus (Supplementary Figure 4). Only Yr7 and Yr5 proteins encode multiple

85   LRR motifs at the C-terminus (Figure 2a; green bars), YrSP having lost most of the LRR

86   region due to the presence of the premature termination codon in exon 3. YrSP still confers

87   functional resistance to *Pst*, although with a different recognition specificity to Yr5. Yr7 and

88   Yr5/YrSP are highly conserved in the N-terminus, with a single amino-acid change in the

89   BED domain. This high degree of conservation is eroded downstream of the BED domain

90   (Figure 2a). The BED domain is required for *Yr7*-mediated resistance, as a single amino acid

91   change in mutant line Cad0903 led to a susceptible reaction (Figure 1a). However,

92   recognition specificity is not solely governed by the BED domain, as the *Yr5* and *YrSP* alleles

93   have identical BED domain sequences, yet confer resistance to different *Pst* isolates. The

4

94 highly conserved Yr7 and Yr5/YrSP BED domains could function in a similar way to the

95 integrated WKRY domain in the *Arabidopsis* RRS1-R immune receptor which binds

96 unrelated bacterial effectors yet activates defense response through mechanisms involving

97 other regions of the protein[23].

98

99 We examined the allelic variation in *Yr7*, *Yr5*, and *YrSP* across eight sequenced tetraploid

100 and hexaploid wheat genomes (Supplementary Table 5). We identified *Yr7* only in Cadenza

101 and Paragon, which are identical-by-descent in this interval (Supplementary File 3,

102 Supplementary Table 6, and Supplementary Figure 5). Both cultivars are derived from the

103 original source of *Yr7*, tetraploid durum wheat (*T. turgidum* ssp. *durum*) cultivar Iumillo and

104 its hexaploid derivative Thatcher (Supplementary Figure 5). None of the three sequenced

105 tetraploid accessions (Svevo, Kronos, Zavitan) carry *Yr7* (Supplementary Table 6).

106

107 For *Yr5/YrSP*, we identified three additional alleles in the sequenced hexaploid wheat

108 cultivars (Figure 2b; Supplementary Table 7). Cultivar Claire encodes a complete NLR with

109 six amino-acid changes, including one within the NB-ARC domain, and six polymorphisms

110 in the C-terminus compared to Yr5. Cultivars Robigus, Paragon, and Cadenza also encode a

111 full length NLR that shares common polymorphisms with Claire, in addition to 19 amino acid

112 substitutions across the BED and NB-ARC domains. The C-terminus polymorphisms

113 between Yr5 and the other cultivars is due to a 774 bp insertion in *Yr5*, close to the 3' end,

114 which carries an alternate termination codon (Supplementary File 2). Tetraploid cultivars

115 Kronos and Svevo encode a fifth Yr5/YrSP allele with a truncation in the LRR region distinct

116 from YrSP, in addition to multiple amino acid substitutions across the C-terminus

117 (Supplementary Table 7). This truncated tetraploid allele is reminiscent of YrSP and is

118 expressed in Kronos (see Methods). However, none of these cultivars (Claire, Robigus,

119   Paragon, Cadenza, Svevo, and Kronos) exhibit a *Yr5/YrSP* resistance response, suggesting

120   that these amino acid changes and truncations may alter recognition specificity or protein

121   function.

122

123   We designed diagnostic markers for *Yr7*, *Yr5*, and *YrSP* to facilitate their detection and use in

124   breeding. We confirmed their presence in the donor cultivars Thatcher and Lee (*Yr7*),

125   Spaldings Prolific (*YrSP*), and spelt wheat cv. Album (*Yr5*) (Supplementary Tables 8-9;

126   Supplementary Figures 5-6). We tested *Yr7* and *YrSP* markers in a collection of global

127   landraces[24] and European cultivars[25] released over the past one hundred years. *YrSP* was

128   absent from the tested germplasm, except for AvocetS-*YrSP* (Supplementary Table 9). *Yr7* on

129   the otherhand was more prevalent in the germplasm tested and we could track its presence

130   across pedigrees, including Cadenza derived cultivars (Supplementary Tables 8-9;

131   Supplementary Figure 5). We confirmed *Yr5* in the AvocetS-*Yr5* and Lemhi-*Yr5* lines and it

132   was not detected in the other tested lines, consistent with the fact that *Yr5* has not yet been

133   deployed within European breeding programmes (Supplementary Tables 10 and 17 and

134   Supplementary Figure 6). The *Yr5* diagnostic marker will facilitate its deployment, hopefully

135   within a breeding strategy that ensures its effectiveness long-term[26].

136

137   We defined the *Yr7/Yr5/YrSP* syntenic interval across the wheat genomes and related grass

138   species *Aegilops tauschii* (D genome progenitor), *Hordeum vulgare* (barley), *Brachypodium*

139   *distachyon*, and *Oryza sativa* (rice) (Supplementary files 4 and 5, Supplementary Figure 7).

140   We identified both canonical NLRs, as well as BED-NLRs across all genomes and species,

141   except for barley, which only contained canonical NLRs across the syntenic region. The

142   phylogenetic relationship based on the NB-ARC domain suggests a common evolutionary

143   origin of these integrated domain NLR proteins before the wheat-rice divergence (~50 Mya)

144   and an expansion in the number of NLRs in the A and B genomes of polyploid wheat species

145   (Figure 3a; Supplementary Figure 8). Within the interval we also identified several genes in

146   the A, B, and D genomes that encode two consecutive in-frame BED domains (named BED-I

147   and BED_II; Figure 3b-c, Supplementary Figure 7) followed by the canonical NLR. The

148   BED domains in these genes were fully encoded within a single exon (exons 2 and 3) and in

149   most cases had a four-exon structure (Figure 3c). This is consistent with the three-exon

150   structure of single BED domain genes, such as *Yr7* and *Yr5/YrSP* (BED-I encoded on exon

151   2). To our knowledge this is the first report of the double BED domain NLR protein

152   structure. The biological function of this molecular innovation remains to be determined,

153   although our data show that the single BED-I structure can confer *Pst* resistance and is

154   required for *Yr7*-mediated resistance.

155

156   Among other mechanisms, integrated domains of NLRs are hypothesised to act as decoys for

157   pathogen effector targets[5]. This would suggest that the integrated domain might be sequence-

158   related to the host protein targeted by the effector. To identify these potential effector targets

159   in the host, we retrieved all BED-domain proteins (108) from the hexaploid wheat genome,

160   including 25 BED-NLRs, and additional BED-NLRs located in the syntenic intervals

161   (Supplementary Table 11; Supplementary file 4). We also retrieved the rice Xa1[10,11] and

162   ZBED proteins, the latter being hypothesized to mediate rice resistance to

163   *Magnaporthe oryzae*[7]. We used the split network method implemented in SplitsTree4[27] to

164   represent the relationships between these BED domains (Figure 3d; Supplementary Figure 9).

165   Overall, BED domains are diverse, although there is evidence of a split between BED

166   domains from BED-NLRs and non-NLR proteins (only 7 of 83 non-NLRs clustered with the

167   BED-NLRs). Given that the base of the split is broad, integrated BED-domains most likely

168   derive from multiple integration events. However, Yr7 and Yr5/YrSP both arose from a

7

169   common integration event that occurred before the *Brachypodium*-wheat divergence

170   (Supplementary Figure 9, purple). This is consistent with the hypothesis that integrated

171   domains might have evolved to strengthen the interaction with pathogen effectors after

172   integration[28], although we cannot exclude the potential role of the BED domains in signalling

173   at this stage.

174

175   Among BED-NLRs, BED-I and BED-II constitute two major clades, consistent with their

176   relatively low amino acid conservation (Figure 3b), that are comprised solely of genes from

177   within the *Yr7/Yr5/YrSP* syntenic region. Seven non-NLR BED domain wheat proteins

178   clustered with BED-NLRs. These are most closely related to the *Brachypodium* and rice

179   BED-NLR proteins and were not expressed in RNA-Seq data from a *Yr5* time-course (re-

180   analysis of published data[29]; Supplementary Figure 10, Supplementary Table 12). Similarly,

181   no BED-containing protein was differentially expressed during this infection time-course,

182   consistent with the prediction that effectors alter their targets' activity at the protein level in

183   the integrated-decoy model[5]. We cannot however disprove that these closely related BED-

184   containing proteins are involved in BED-NLR-mediated resistance.

185

186   BED-NLRs are frequent in Triticeae, and occur in other monocot and dicot tribes[6–8]. To date

187   a single BED-NLR gene, *Xa1*, has been shown to confer resistance to plant pathogens[10,11]. In

188   the present study, we show that the distinct *Yr7*, *Yr5*, and *YrSP* resistance specificities belong

189   to a complex NLR cluster on chromosome 2B and are encoded by two paralogous BED-

190   NLRs genes. We report an allelic series for the *Yr5/YrSP* gene with five independent alleles,

191   including three full-length BED-NLRs (including *Yr5*) and two truncated versions (including

192   *YrSP*). This wider allelic series could be of functional significance as previously shown for

193   the *Mla* and *Pm3* loci that confer resistance to *Blumeria graminis*[22,30] in barley and wheat,

8

194   respectively, and the flax *L* locus conferring resistance to *Melampsora lini*[31]. Overall, our

195   results add strong evidence for the importance of the BED-NLR architecture in plant-

196   pathogen interactions. The paralogous and allelic relationship of these three distinct *Yr* loci

197   will inform future hypothesis-driven engineering of novel recognition specificities.

198 **Methods**

199 **MutRenSeq**

200 *Mutant identification*

201 Supplementary Table 3 summarises plant materials and *Pst* isolates used to identify mutants

202 for each *Yr* gene. We used an EMS-mutagenised population in cultivar Cadenza[32] to identify

203 mutants in *Yr7*; whereas EMS-populations in the corresponding AvocetS-*Yr* near isogenic

204 line (NIL) were used to identify *Yr5* and *YrSP* mutants. For *Yr7*, we inoculated M_3 plants

205 from the Cadenza EMS population with *Pst* isolate 08/21 which is virulent to *Yr1, Yr2, Yr3,*

206 *Yr4, Yr6, Yr9, Yr17, Yr27, Yr32, YrRob,* and *YrSol*[33]. We hypothesised that susceptible

207 mutants would carry mutations in *Yr7*. Plants were grown in 192-well trays in a confined

208 glasshouse with no supplementary lights or heat. Inoculations were performed at the one leaf

209 stage (Zadoks 11) with a talc – urediniospore mixture. Trays were kept in darkness at 10 °C

210 and 100% humidity for 24 hours. Infection types (IT) were recorded 21 days post-inoculation

211 (dpi) following the Grassner and Straib scale[34]. Identified susceptible lines were progeny

212 tested to confirm the reliability of the phenotype and DNA from M_4 plants was used for

213 RenSeq (see section below). Similar methods were used for AvocetS-*Yr7*, AvocetS-*Yr5*, and

214 AvocetS-*YrSP* EMS-mutagenised populations with the following exceptions: *Pst* pathotypes

215 108 E141 A+ (University of Sydney Plant Breeding Institute Culture no. 420), 150 E16 A+

216 (Culture no. 598) and 134 E16 A+ (Culture no. 572) were used to evaluate *Yr7, Yr5*, and

217 *YrSP* mutants, respectively. EMS-derived susceptible mutants in Lemhi-*Yr5* were previously

218 identified[35] and DNA from M_5 plants was used for RenSeq.

219

220 *DNA preparation, resistance gene enrichment and sequencing (RenSeq)*

221 We extracted total genomic DNA from young leaf tissue using the large-scale DNA

222 extraction protocol from the McCouch Lab (https://ricelab.plbr.cornell.edu/dna_extraction)

223 and a previously described method[36]. We checked DNA quality and quantity on a 0.8%

224 agarose gel and with a NanoDrop spectrophotometer (Thermo Scientific). Arbor Biosciences

225 (Ann Arbor, MI, USA) performed the targeted enrichment of NLRs according to the MYbaits

226 protocol using an improved version of the previously published Triticeae bait library

227 available at github.com/steuernb/MutantHunter. Library construction was performed using

228 the TruSeq RNA protocol v2 (Illumina 15026495). Libraries were pooled with one pool of

229 samples for Cadenza mutants and one pool of eight samples for the Lemhi-*Yr5* parent and

230 Lemhi-*Yr5* mutants. AvocetS-*Yr5* and AvocetS-*YrSP* wild-type, together with their respective

231 mutants, were also processed according to the MYbaits protocol and the same bait library

232 was used. All enriched libraries were sequenced on a HiSeq 2500 (Illumina) in High Output

233 mode using 250 bp paired end reads and SBS chemistry. For the Cadenza wild-type, we

234 generated data on an Illumina MiSeq instrument. In addition to the mutants, we also

235 generated RenSeq data for Kronos and Paragon to assess the presence of *Yr5* in Kronos and

236 *Yr7* in Paragon. Details of all the lines sequenced, alongside NCBI accession numbers, are

237 presented in Supplementary Tables 3 and 12.

238

239 **MutantHunter pipeline**

240 We adapted the pipeline from https://github.com/steuernb/MutantHunter/ to identify

241 candidate contigs for the targeted *Yr* genes. First, we trimmed the RenSeq-derived reads with

242 trimmomatic[37] using the following parameters: ILLUMINACLIP:TruSeq2-PE.fa:2:30:10

243 LEADING:30 TRAILING:30 SLIDINGWINDOW:10:20 MINLEN:50 (v0.33). We made *de*

244 *novo* assemblies of wild-type plant trimmed reads with the CLC assembly cell and default

245 parameters apart from the word size (-w) parameter that we set to 64 (v5.0,

246 http://www.clcbio.com/products/clc-assembly-cell/) (Supplementary Table 14). We then

247 followed the MutantHunter pipeline detailed at https://github.com/steuernb/MutantHunter/.

11

248   For Cadenza mutants, we used the following MutantHunter program parameters to identify

249   candidate contigs: -c 20 -n 6 -z 1000. These options require a minimum coverage of 20x for

250   SNPs to be called; at least six susceptible mutants must have a mutation in the same contig to

251   report it as candidate; small deletions were filtered out by setting the number of coherent

252   positions with zero coverage to call a deletion mutant at 1000. The -n parameter was

253   modified accordingly in subsequent runs with the Lemhi-*Yr5* datasets (-n 6).

254

255   To identify *Yr5* and *YrSP* contigs from Avocet mutants, we followed the MutantHunter

256   pipeline with all default parameters, except in the use of CLC Genomics Workbench (v10)

257   for reads QC, trimming, *de novo* assembly of Avocet wild-type and mapping all the reads

258   against *de novo* wild-type assembly. The default MutantHunter parameters were used except

259   that –z was set as 100. The parameter –n was set to 2 in the first run and then to 3 in the

260   second run. Two *Yr5* mutants were most likely sibling lines as they carried identical

261   mutations at the same position (Supplementary Figure 2, Supplementary Table 4).

262

263   For *Yr7* we identified a single contig with six mutations, however we did not identify

264   mutations in line Cad0903. Upon examination of the *Yr7* candidate contig we predicted that

265   the 5' region was likely to be missing (Supplementary Figure 2). We thus annotated potential

266   NLRs in the Cadenza genome assembly available from the Earlham Institute (Supplementary

267   Table 5, http://opendata.earlham.ac.uk/Triticum_aestivum/EI/v1.1) with the NLR-Annotator

268   program using default parameters (https://github.com/steuernb/NLR-Annotator). We

269   identified an annotated NLR in the Cadenza genome with 100% sequence identity to the *Yr7*

270   candidate contig, which extended beyond our *de novo* assembled sequence. We therefore

271   replaced the previous candidate contig with the extended Cadenza sequence (100% sequence

272   identity) and mapped the RenSeq reads from Cadenza wild-type and mutants as described

273   above. This confirmed the candidate contig for *Yr7* as we retrieved the missing 5' region

274   including the BED domain. The improved contig now also contained a mutation in the

275   outstanding mutant line Cad0903 (Supplementary Figure 2). The Triticeae bait library does

276   not include integrated domains in its design so they are prone to be missed, especially when

277   located at the ends of an NLR. Sequencing technology could also have accounted for this:

278   MiSeq was used for Cadenza wild-type whereas HiSeq was chosen for Lemhi-*Yr5* and we

279   recovered the 5' region in the latter, although coverage was lower than for the regions

280   encoding canonical domains. In summary, we sequenced nine, ten, and four mutants for *Yr7*,

281   *Yr5,* and *YrSP,* respectively and identified for each target gene a single contig that accounted

282   for all mutants.

283

284   **Candidate contig confirmation and gene annotation**

285   We sequenced the *Yr7, Yr5,* and *YrSP* candidate contigs from the mutant lines (annotated in

286   Supplementary Files 1 and 2) to confirm the EMS-derived mutations using primers

287   documented in Supplementary Table 15. We first PCR-amplified the complete locus from the

288   same DNA preparations as the ones submitted for RenSeq with the Phusion® High-Fidelity

289   DNA Polymerase (New England Biolabs) following the suppliers protocol

290   (https://www.neb.com/protocols/0001/01/01/pcr-protocol-m0530). We then carried out

291   nested PCR on the obtained product to generate overlapping 600-1,000 bp amplicons that

292   were purified using the MiniElute kit (Qiagen). The purified PCR products were sequenced

293   by GATC following the LightRun protocol (https://www.gatc-biotech.com/shop/en/lightrun-

294   tube-barcode.html). Resulting sequences were aligned to the wild-type contig using

295   ClustalOmega (https://www.ebi.ac.uk/Tools/msa/clustalo/). This allowed us to curate the *Yr7*

296   locus in the Cadenza assembly that contained two sets of unknown ('N') bases in its

13

297   sequence, corresponding to a 39 bp insertion and a 129 bp deletion (Supplementary File 3),

298   and to confirm the presence of the mutations in each mutant line.

299   We used HISATt2[38] (v2.1) to map RNA-Seq reads available from Cadenza and AvocetS-

300   Yr5[29] to the RenSeq *de novo* assemblies with curated loci to define the structure of the genes.

301   We used the following parameters: --no-mixed --no-discordant to map reads in pairs only.

302   We used the --novel-splicesite-outfile to predict splicing sites that we manually scrutinised

303   with the genome visualisation tool IGV[39] (v2.3.79). Predicted coding sequences (CDS) were

304   translated using the ExPASy online tool (https://web.expasy.org/translate/). This allowed us

305   to predict the effect of the mutations on each candidate transcript (Figure 1a; Supplementary

306   Table 4). The long-range primers for both *Yr7* and *Yr5* loci were then used on the

307   corresponding susceptible Avocet NIL mutants to determine whether the genes were present

308   and carried mutations in that background (Figure 1a; Supplementary Files 1 and 2).

309

Coiled coil domain prediction

311   To determine whether *Yr7*, *Yr5*, and *YrSP* encode Coiled Coil (CC) domains we used the

312   NCOILS prediction program[40] (v1.0, https://embnet.vital-it.ch/software/COILS_form.html)

313   with the following parameters: MTIK matrix with applying a 2.5-fold weighting of positions

314   a,d. We compared the profiles to those obtained with already characterised CC-NLR

315   encoding genes *Sr33*, *Mla10*, *Pm3* and *RPS5* (Supplementary Figure 4). We also ran the

316   program on Yr7 and Yr5 protein sequences where the BED domain was manually removed to

317   determine whether its integration could have disrupted an existing CC domain. To further

318   investigate whether *Yr7*, *Yr5*, and *YrSP* encode CC domains we performed a BLASTP

319   analysis[41] with their N-terminal region, from the methionine to the first amino acid encoding

320   the NB-ARC domain, with or without the BED domain (Supplementary Figure 4).

321

14

Genetic linkage

We generated a set of F_2 populations to genetically map the candidate contigs (Supplementary Table 3). For *Yr7* we developed an F_2 population based on a cross between the susceptible mutant line Cad0127 to the Cadenza wild-type (population size 139 individuals). For *Yr5* and *YrSP* we developed F_2 populations between AvocetS and the NILs carrying the corresponding *Yr* gene (94 individuals for *YrSP* and 376 for *Yr5*). We extracted DNA from leaf tissue at the seedling stage (Zadoks 11) following a previously published protocol[42] and Kompetitive Allele Specific PCR (KASP) assays were carried out as described in[43]. R/qtl package[44] was used to produce the genetic map based on a general likelihood ratio test and genetic distances were calculated from recombination frequencies (v1.41-6).

We used previously published markers linked to *Yr7*, *Yr5*, and *YrSP* (WMS526, WMS501 and WMC175, WMC332, respectively[15,18,19]) in addition to closely linked markers WMS120, WMS191, and WMC360 (based on the GrainGenes database https://wheat.pw.usda.gov/GG3/) to define the physical region on the Chinese Spring assembly RefSeq v1.0 (https://wheat-urgi.versailles.inra.fr/Seq-Repository/Assemblies). Two different approaches were used for genetic mapping depending on the material. For *Yr7*, we used the public data[32] for Cad0127 (www.wheat-tilling.com) to identify nine mutations located within the *Yr7* physical interval based on BLAST analysis against RefSeq v1.0. We used KASP primers when available and manually designed additional ones including an assay targeting the Cad0127 mutation in the *Yr7* candidate contig (Supplementary Table 15). We genotyped the Cad0127 F_2 populations using these nine KASP assays and confirmed genetic linkage between the Cad0127 *Yr7* candidate mutation and the nine mutations across the physical interval (Supplementary Figure 3).

15

347   For *Yr5* and *YrSP*, we first aligned the candidate contigs to the best BLAST hit in an AvocetS

348   RenSeq *de novo* assembly. We then designed KASP primers targeting polymorphisms

349   between these sequences and used them to genotype the corresponding F_2 population

350   (Supplementary Table 15). For both candidate contigs we confirmed genetic linkage with the

351   previously published genetic intervals for these *Yr* genes (Supplementary Figure 3).

352

353   ***Yr7* gene-specific markers**

354   We aligned the *Yr7* sequence with the best BLAST hits in the genomes listed on

355   Supplementary Table 5 and designed KASP primers targeting polymorphisms that were *Yr7*-

356   specific. Three markers were retained after testing on a selected panel of Cadenza-derivatives

357   and cultivars that were positive for *Yr7* markers in the literature, including the *Yr7* reference

358   cultivar Lee (Supplementary Table 8, 8 and 15). The panel of Cadenza-derivatives was

359   phenotyped with three *Pst* isolates: *Pst* 08/21 (*Yr7*-avirulent), *Pst* 15/151 (*Yr7*-avirulent –

360   virulent to *Yr1, 2, 3, 4, 6, 9, 17, 25, 32, Rendezvous, Sp, Robigus, Solstice*) and *Pst* 14/106

361   (*Yr7*-virulent, virulent to *Yr1, 2, 3, 4, 6, 7, 9, 17, 25, 32, Sp, Robigus, Solstice ,Warrior,*

362   *Ambition, Cadenza, KWS Sterling, Apache*) to determine whether *Yr7*-positive cultivars, as

363   identified by the three KASP markers, displayed a consistent specificity (Supplementary

364   Table 8). Pathology assays were performed as for the screening of the Cadenza mutant

365   population. We retrieved pedigree information for the analysed cultivars from the Genetic

366   Resources   Information   System   for   Wheat   and   Triticale   database   (GRIS,

367   www.wheatpedigree.net) and used the Helium software[45] (v1.17) to illustrate the breeding

368   history of *Yr7* in the UK (Supplementary Figure 5).

369

370   We used the three *Yr7* KASP markers to genotype (i) cultivars from the AHDB Wheat

371   Recommended   List   from   2005-2018   (https://cereals.ahdb.org.uk/varieties/ahdb-

16

372   recommended-lists.aspx); (ii) the Gediflux collection of European bread wheat cultivars

373   released between 1920 and 2010[25] and (iii) the core Watkins collection, which represents a

374   global set of wheat landraces collected in the 1930s[24]. Results are reported in Supplementary

375   Table 9.

376

377   **_Yr5_ and _YrSP_ gene-specific markers**

378   We identified a 774 bp insertion in the _Yr5_ allele 29 bp upstream of the STOP codon with

379   respect to the Cadenza and Claire alleles. Genomic DNA from _YrSP_ confirmed that the

380   insertion was specific to _Yr5_. We used this polymorphism to design primers flanking the

381   insertion and tested them on a subset of the collections mentioned above. We added 32 DNA

382   sample from diverse accessions of _Triticum dicoccoides,_ the wild progenitor of domesticated

383   wheat (passport data shown in Supplementary Table 17). We included DNA from _Triticum_

384   _aestivum_ ssp. _spelta_ var. album[35] (_Yr5_ donor) and Spaldings Prolific (_YrSP_ donor) to assess

385   their amplification profiles. PCR amplification was conducted using a touchdown

386   programme: 10 cycles, -0.5 °C per cycle starting from 67 °C and the remaining 25 cycles at

387   62 °C. This allowed us to increase the specificity of the reaction. We observed three different

388   profiles on the tested varieties; (i) a 1,281 bp amplicon in _Yr5_ positive cultivars, (ii) a 507 bp

389   amplicon in the alternate _Yr5_ allele carriers, including AvocetS-_YrSP_, Cadenza, and Claire,

390   and (iii) no amplification in other varieties. We sequenced the different amplicons and

391   confirmed the insertion in _Yr5_ compared to the alternate alleles (Supplementary File 2). The

392   lack of amplicons in some varieties most likely respresents the absence of the loci in the

393   tested varieties. For _YrSP_, we aligned the _YrSP_ and _Yr5_ sequences to design KASP primers

394   targeting the G to C SNP between the two alleles (Supplementary File 2, Supplementary

395   Table 16). We tested the marker by genotyping selected cultivars as controls and cultivars

396   from the AHDB Wheat Recommended List from 2005-2018 (Supplementary Table 9).

17

397

398 ***In silico* allele mining for *Yr7* and *Yr5***

399 We used the *Yr7* and *Yr5* sequences to retrieve the best BLAST hits in the *T. aestivum* and *T.*

400 *turgdium* wheat genomes listed in Supplementary Table 5. The best *Yr5* hits shared between

401 93.6 and 99.3% sequence identity, which was comparable to what was observed for alleles

402 derived from the wheat *Pm3* (>97% identity)[46] and flax *L* (>90% identity)[31] genes. *Yr7* was

403 identified only in Paragon and Cadenza (Supplementary Table 6; See Supplementary File 3

404 for curation of the Paragon sequence).

405

406 **Analysis of the *Yr7* and *Yr5*/*YrSP* cluster on RefSeq v1.0**

407 *Definition of syntenic regions across grass genomes*

408 We used NLR-Annotator to identify putative NLR loci on RefSeq v1.0 chromosome 2B and

409 identified the best BLAST hits to *Yr7* and *Yr5* on RefSeq v1.0. Additional BED-NLRs and

410 canonical NLRs were annotated in close physical proximity to these best BLAST hits.

411 Therefore, to better define the NLR cluster we selected ten non-NLR genes located both

412 distal and proximal to the region, and identified orthologs in barley, *Brachypodium,* and rice

413 in *EnsemblPlants* (https://plants.ensembl.org/). We used different % ID cutoffs for each

414 species (>92% for barley, >84% for *Brachypodium*, and >76% for rice) and determined the

415 syntenic region when at least three consecutive orthologues were found. A similar approach

416 was conducted for *Triticum* ssp and *Ae. tauschii* (Supplementary file 4).

417

418 *Definition of the NLR content of the syntenic region*

419 We extracted the previously defined syntenic region from the grass genomes listed in

420 Supplementary Table 5 and annotated NLR loci with NLR-Annotator. We maintained

421 previously defined gene models where possible, but also defined new gene models that were

18

422 further analysed through a BLASTx analysis to confirm the NLR domains (Supplementary

423 Files 4 and 5). The presence of BED domains in these NLRs was also confirmed by CD-

424 Search (https://www.ncbi.nlm.nih.gov/Structure/cdd/wrpsb.cgi).

425

426 **Phylogenetic and neighbour network analyses**

427 We aligned the translated NB-ARC domains from the NLR-Annotator output with

428 MUSCLE[47] using default parameters (v.3.8.31). We verified and manually curated the

429 alignment with Jalview[48] (v2.10.1). We used Gblocks[49] (v0.91b) with the following

430 parameters: Minimum Number Of Sequences For A Conserved Position: 9; Minimum

431 Number Of Sequences For A Flanking Position: 14; Maximum Number Of Contiguous

432 Nonconserved Positions: 8; Minimum Length Of A Block: 10; Allowed Gap Positions: None;

433 Use Similarity Matrices: Yes; to eliminate poorly aligned positions. This resulted in 36% of

434 the original 156 positions being taken forward for the phylogeny. We built a Maximum

435 Likelihood tree with the RAxML[50] program and the following parameters: raxmlHPC -f a -x

436 12345 -p 12345 -N 1000 -m PROTCATJTT -s <input_alignment.fasta> (MPI version

437 v8.2.10). The best scoring tree with associated bootstrap values was visualised and mid-

438 rooted with Dendroscope[51] (v3.5.9). There was clear separation between NLRs belonging to

439 the two different clusters but the sub-clades had less support. One explanation would be that

440 conflicting phylogenetic signals that are due to events such as hybridization, horizontal gene

441 transfer, recombination, or gene duplication and loss might have occurred in the region. Split

442 networks allow nodes that do not represent ancestral species and can thus represent such

443 incompatible and ambiguous signals. We therefore used this method in the following part of

444 the analysis to analyse the relationship between the BED domains.

445

446   We used the Neighbour-net method[52] implemented in SplitsTree4[27] (v4.16) to analyse the

447   relationships between BED domains from NLR and non-NLR proteins. First we retrieved all

448   BED-containing proteins from RefSeq v1.0 using the following steps: we used hmmer

449   (v3.1b2, http://hmmer.org/) to identify conserved domains in protein sequences from RefSeq

450   v1.0. We applied a cut-off of 0.01 on i-evalue to filter out any irrelevant identified domains.

451   We separated the set between NLR and non-NLRs based on the presence of the NB-ARC and

452   sequence homology for single BED proteins. BED domains were extracted from the

453   corresponding protein sequences based on the hmmer output and were verified on the CD-

454   search database. Alignments of the BED domains were performed in the same way as for

455   NB-ARC domains and were used to generate a neighbour network in SplitsTree4 based on

456   the uncorrected P distance matrix.

457

458   **Transcriptome analysis**

459   *Kronos analysis*

460   We reanalysed RNA-Seq data from cultivar Kronos[53] to determine whether the Kronos *Yr5*

461   allele was expressed. We followed the same strategy as that described to define the *Yr7* and

462   *Yr5* gene structures (candidate contig confirmation and gene annotation section). We

463   generated a *de novo* assembly of the Kronos NLR repertoire from Kronos RenSeq data and

464   used it as a reference when mapping read data from one replicate of the wild-type Kronos at

465   heading stage. Read depths up to 30x were present for the *Yr5* allele which allowed

466   confirmation of its expression. Likewise, the RNA-Seq reads confirmed the gene structure,

467   which is similar to *YrSP*, and the premature termination codon in Kronos *Yr5*. Whether this

468   allele confers resistance against *Pst* remains to be elucidated.

469

470   *Re-analysis of RNA-Seq data in Dobon et al., 2016*

471   We used RNA-Seq data previously published by Dobon and colleagues[18]. Briefly, two RNA-

472   Seq time-courses were used based on samples taken from leaves at 0, 1, 2, 3, 5, 7, 9, and 11

473   dpi for the susceptible cultivar Vuka and 0, 1, 2, 3, and 5 dpi for the resistant AvocetS-*Yr5*[29].

474   We used normalised read counts (Transcript Per Million, TPM) from Ramirez-Gonzalez et al.

475   2018 to produce the heatmap shown in Supplementary Figure 10 with the pheatmap R

476   package[54] (v1.0.8). Transcripts were clustered according to their expression profile as defined

477   by a Euclidean distance matrix and hierarchical clustering. Transcripts were considered

478   expressed if their average TPM was $\geq$0.5 TPM in at least one time point. We used the

479   DESeq2 R package[55] (v1.18.1) to conduct a differential expression analysis. We performed

480   two comparisons: (1) we used a likelihood ratio test to compare the full model ~ Cultivar +

481   Time + Cultivar:Time to the reduced model ~ Cultivar + Time to identify genes that were

482   differentially expressed between the two cultivars at a given time point after 0 dpi (workflow:

483   https://www.bioconductor.org/help/workflows/rnaseqGene/); (2) Investigation of both time

484   courses in Vuka and AvocetS-*Yr5* independently to generate all of the comparisons between

485   0 dpi and any given time point, following the standard DESeq2 pipeline. Genes were

486   considered as differentially expressed genes if they showed an adjusted p-value < 0.05 and a

487   log2 fold change of 2 or higher. Most BED-containing proteins and BED-NLRs were not

488   expressed in the analysed data. No pattern was observed for those that were expressed:

489   differences were observed between cultivars, but these were independent of the presence of

490   the yellow rust pathogen.

491

References

493   1.   Oerke, E. C. Crop losses to pests. *J. Agric. Sci.* **144,** 31–43 (2006).

494   2.   Hubbard, A. *et al.* Field pathogenomics reveals the emergence of a diverse wheat
495   yellow rust population. *Genome Biol.* **16,** 23 (2015).

496   3.   Aravind, L. The BED finger, a novel DNA-binding domain in chromatin-boundary-
497   element-binding proteins and transposases. *Trends Biochem. Sci.* **25,** 421–423 (2000).

21

498   4.   Jones, J. D. G. & Dangl, J. L. The plant immune system. *Nature* **444,** 323–329 (2006).

499   5.   Kourelis, J. & van der Hoorn, R. A. L. Defended to the nines: 25 years of resistance
500   gene cloning identifies nine mechanisms for R protein function. *Plant Cell* (2018).
501   doi:10.1105/tpc.17.00579

502   6.   Sarris, P. F., Cevik, V., Dagdas, G., Jones, J. D. G. & Krasileva, K. V. Comparative
503   analysis of plant immune receptor architectures uncovers host proteins likely targeted
504   by pathogens. *BMC Biol.* **14,** 8 (2016).

505   7.   Kroj, T., Chanclud, E., Michel-Romiti, C., Grand, X. & Morel, J.-B. Integration of
506   decoy domains derived from protein targets of pathogen effectors into plant immune
507   receptors is widespread. *New Phytol.* **210,** 618–626 (2016).

508   8.   Bailey, P. C. *et al.* Dominant integration locus drives continuous diversification of
509   plant immune receptors with exogenous domain fusions. *Genome Biol.* **19,** 23 (2018).

510   9.   Bundock, P. & Hooykaas, P. An *Arabidopsis* hAT-like transposase is essential for
511   plant development. *Nature* **436,** 282–284 (2005).

512   10. Yoshimura, S. *et al.* Expression of *Xa1*, a bacterial blight-resistance gene in rice, is
513   induced by bacterial inoculation. *Proc. Natl. Acad. Sci. U. S. A.* **95,** 1663–1668 (1998).

514   11. Das, B., Sengupta, S., Prasad, M. & Ghose, T. Genetic diversity of the conserved
515   motifs of six bacterial leaf blight resistance genes in a set of rice landraces. *BMC
516   Genet.* **15,** 82 (2014).

517   12. Law, C. N. Genetic control of yellow rust resistance in *T. spelta* Album. *Plant Breed.
518   Institute, Cambridge, Annu. Rep.* **1975,** 108–109 (1976).

519   13. Johnson, R. & Dyck, P. L. Resistance to yellow rust in *Triticum spelta* var. Album and
520   bread wheat cultivars Thatcher and Lee. *Colloq. l'INRA* (1984).

521   14. Zhang, P., McIntosh, R. A., Hoxha, S. & Dong, C. M. Wheat stripe rust resistance
522   genes *Yr5* and *Yr7* are allelic. *Theor. Appl. Genet.* **120,** 25–29 (2009).

523   15. Feng, J. Y. *et al.* Molecular mapping of *YrSP* and its relationship with other genes for
524   stripe rust resistance in wheat chromosome 2BL. *Phytopathology* **105,** 1206–1213
525   (2015).

526   16. Zhan, G. *et al.* Virulence and molecular diversity of the *Puccinia striiformis* f. sp.
527   *tritici* population in Xinjiang in relation to other regions of western China. *Plant Dis.*
528   **100,** 99–107 (2016).

529   17. Steuernagel, B. *et al.* Rapid cloning of disease-resistance genes in plants using
530   mutagenesis and sequence capture. *Nat. Biotechnol.* **34,** 652–655 (2016).

531   18. Sun, Q., Wei, Y., Ni, Z., Xie, C. & Yang, T. Microsatellite marker for yellow rust
532   resistance gene *Yr5* in wheat introgressed from spelt wheat. *Plant Breed.* **121,** 539–541
533   (2002).

534   19. Yao, Z. J. *et al.* The molecular tagging of the yellow rust resistance gene *Yr7* in wheat
535   transferred from differential host Lee using microsatellite markers. *Sci. Agric. Sin.* **39,**
536   1146–1152 (2006).

537   20. Bai, S. *et al.* Structure-function analysis of barley NLR immune receptor MLA10
538   reveals its cell compartment specific activity in cell death and disease resistance. *PLoS
539   Pathog.* **8,** e1002752 (2012).

540   21. Periyannan, S. *et al.* The gene *Sr33*, an ortholog of barley *Mla* genes, encodes

541   resistance to wheat stem rust race Ug99. *Science.* **341,** 786–788 (2013).

542   22. Srichumpa, P., Brunner, S., Keller, B. & Yahiaoui, N. Allelic series of four powdery
543   mildew resistance genes at the Pm3 locus in hexaploid bread wheat. *Plant Physiol.*
544   **139,** 885–895 (2005).

545   23. Sarris, P. F. *et al.* A plant immune receptor detects pathogen effectors that target
546   WRKY transcription factors. *Cell* **161,** 1089–1100 (2015).

547   24. Wingen, L. U. *et al.* Establishing the A. E. Watkins landrace cultivar collection as a
548   resource for systematic gene discovery in bread wheat. *Theor. Appl. Genet.* **127,** 1831–
549   1842 (2014).

550   25. Reeves, J. C. *et al.* Changes over time in the genetic diversity of four major European
551   crops - a report from the Gediflux Framework 5 project. *Genet. Var. plant breeding.*
552   *Proc. 17th EUCARPIA Gen. Congr. Tulln, Austria, 8-11 Sept. 2004* 3–7 (2004).

553   26. Ellis, J. G., Lagudah, E. S., Spielmeyer, W. & Dodds, P. N. The past, present and
554   future of breeding rust resistant wheat. *Front Plant Sci* **5,** 641 (2014).

555   27. Huson, D. H. & Bryant, D. Application of phylogenetic networks in evolutionary
556   studies. *Mol. Biol. Evol.* **23,** 254–267 (2006).

557   28. Ellis, J. G. Integrated decoys and effector traps: how to catch a plant pathogen. *BMC*
558   *Biol.* **14,** 13 (2016).

559   29. Dobon, A., Bunting, D. C. E., Cabrera-Quio, L. E., Uauy, C. & Saunders, D. G. O. The
560   host-pathogen interaction between wheat and yellow rust induces temporally
561   coordinated waves of gene expression. *BMC Genomics* **17,** 380 (2016).

562   30. Seeholzer, S. *et al.* Diversity at the *Mla* powdery mildew resistance locus from
563   cultivated barley reveals sites of positive selection. *Mol. Plant-Microbe Interact.* **23,**
564   497–509 (2010).

565   31. Ellis, J. G., Lawrence, G. J., Luck, J. E. & Dodds, P. N. Identification of regions in
566   alleles of the flax rust resistance gene *L* that determine differences in gene-for-gene
567   specificity. *Plant Cell* **11,** 495–506 (1999).

568   32. Krasileva, K. V *et al.* Uncovering hidden variation in polyploid wheat. *Proc. Natl.*
569   *Acad. Sci. U. S. A.* **6,** E913–E921 (2017).

570   33. Hubbard, A. J., Fanstone, V. & Bayles, R. A. *UKCPVS 2009 Annual report*.

571   34. Gassner, G. & Straib, W. *Die Bestimmung der biologischen Rassen des*
572   *Weizengelbrostes* Puccinia glumarum f.sp. tritici *Schmidt Erikss. u. Henn.* (1932).

573   35. McGrann, G. R. D. *et al.* Genomic and genetic analysis of the wheat race-specific
574   yellow rust resistance gene *Yr5*. *J. Plant Sci. Mol. Breed.* **3,** (2014).

575   36. Lagudah, E. S., Appels, R., Brown, A. H. D. & McNeil, D. The molecular–genetic
576   analysis of *Triticum tauschii*, the D-genome donor to hexaploid wheat. *Genome* **34,**
577   375–386 (1991).

578   37. Bolger, A. M., Lohse, M. & Usadel, B. Trimmomatic: a flexible trimmer for Illumina
579   sequence data. *Bioinformatics* **30,** 2114–2120 (2014).

580   38. Kim, D., Langmead, B. & Salzberg, S. L. HISAT: a fast spliced aligner with low
581   memory requirements. *Nat. Methods* **12,** 357–360 (2015).

582   39. Thorvaldsdottir, H., Robinson, J. T. & Mesirov, J. P. Integrative Genomics Viewer

583   (IGV): high-performance genomics data visualization and exploration. *Brief.*
584   *Bioinform.* **14,** 178–192 (2013).

585 40. Lupas, A., Dyke, M. Van & Stock, J. Predicting coiled coils from protein sequences.
586   *Science.* **252,** 1162–1164 (1991).

587 41. Altschul, S. F. *et al.* Protein database searches using compositionally adjusted
588   substitution matrices. *FEBS J.* **272,** 5101–9 (2005).

589 42. Pallotta, M. A. *et al.* Marker assisted wheat breeding in the southern region of
590   Australia. in *Proceedings of 10th International Wheat Genet Symposium Instituto*
591   *Sperimentale per la Cerealcoltura Rome* 789–791 (2003).

592 43. Ramirez-Gonzalez, R. H. *et al.* RNA-Seq bulked segregant analysis enables the
593   identification of high-resolution genetic markers for breeding in hexaploid wheat.
594   *Plant Biotechnol J* **13,** 613–624 (2015).

595 44. Broman, K. W., Wu, H., Sen, S. & Churchill, G. A. R/qtl: QTL mapping in
596   experimental crosses. *Bioinformatics* **19,** 889–890 (2003).

597 45. Shaw, P. D., Graham, M., Kennedy, J., Milne, I. & Marshall, D. F. Helium:
598   visualization of large scale plant pedigrees. *BMC Bioinformatics* **15,** 259 (2014).

599 46. Brunner, S. *et al.* Intragenic allele pyramiding combines different specificities of
600   wheat *Pm3* resistance alleles. *Plant J.* **64,** 433–445 (2010).

601 47. Edgar, R. C. MUSCLE: multiple sequence alignment with high accuracy and high
602   throughput. *Nucleic Acids Res.* **32,** 1792–1797 (2004).

603 48. Waterhouse, A. M., Procter, J. B., Martin, D. M. A., Clamp, M. & Barton, G. J.
604   Jalview Version 2--a multiple sequence alignment editor and analysis workbench.
605   *Bioinformatics* **25,** 1189–1191 (2009).

606 49. Castresana, J. Selection of conserved blocks from multiple alignments for their use in
607   phylogenetic analysis. *Mol. Biol. Evol.* **17,** 540–552 (2000).

608 50. Stamatakis, A. RAxML-VI-HPC: maximum likelihood-based phylogenetic analyses
609   with thousands of taxa and mixed models. *Bioinformatics* **22,** 2688–2690 (2006).

610 51. Huson, D. H. & Scornavacca, C. Dendroscope 3: An interactive yool for rooted
611   phylogenetic trees and networks. *Syst. Biol.* **61,** 1061–1067 (2012).

612 52. Bryant, D. & Moulton, V. Neighbor-Net: An agglomerative method for the
613   construction of phylogenetic networks. *Mol. Biol. Evol.* **21,** 255–265 (2003).

614 53. Pearce, S. *et al.* Regulation of Zn and Fe transporters by the GPC1gene during early
615   wheat monocarpic senescence. *BMC Plant Biol.* **14,** 368 (2014).

616 54. Kolde, R. Pheatmap: pretty heatmaps. *R package version* (2015).

617 55. Love, M. I., Huber, W. & Anders, S. Moderated estimation of fold change and
618   dispersion for RNA-seq data with DESeq2. *Genome Biol.* **15,** 550 (2014).

619 56. Jupe, F. *et al.* Identification and localisation of the NB-LRR gene family within the
620   potato genome. *BMC Genomics* **13,** 75 (2012).

621 57. Warren, R. F., Henk, A., Mowery, P., Holub, E. & Innes, R. W. A mutation within the
622   leucine-rich repeat domain of the arabidopsis disease resistance gene RPS5 partially
623   suppresses multiple bacterial and downy mildew resistance genes. *Plant Cell* **10,**
624   1439–1452 (1998).

625 58. Avni, R. *et al.* Wild emmer genome architecture and diversity elucidate wheat
626   evolution and domestication. *Science (80-.).* **357,** 93–97 (2017).
627 59. Luo, M.-C. *et al.* Genome sequence of the progenitor of the wheat D genome *Aegilops*
628   *tauschii*. *Nature* **551,** 498 (2017).

Author contributions

CM performed the experiments to clone *Yr7* and *Yr5* and the subsequent analyses of their loci

and BED domains, designed the gene-specific markers, analysed the genotype data in the

studied panels, and designed and made the figures. JZ performed the experiments to

clone *YrSP*, confirm the *Yr7* and *Yr5* genes in AvocetS-*Yr7* and AvocetS-*Yr5* mutants, and

identified the full length of *Yr5* and *YrSP* with their respective regulatory elements. CM and

JZ developed the gene specific markers. PZ and RM performed the EMS treatment, isolation,

and confirmation of *Yr7, Yr5,* and *YrSP* mutants in AvocetS NILs. PF performed the

pathology work on the Cadenza *Yr7* mutants and the mapping populations. BS helped with

the NLR annotator analysis and provided the bait library for target enrichment and

sequencing of NLRs, NMA provided DNA samples for allelic variation studies and LB

provided Lemhi-*Yr5* mutants. RM, EL, PZ, BW, SB, and CU conceived, designed, and

supervised the research. CM and CU wrote the manuscript. JZ, PZ, RM, BW, NMA, LB and

EL provided edits.

Data availability

All sequencing data has been deposited in the NCBI Short Reads Archive under accession

numbers listed in Supplementary Table 13 (SRP139043). Cadenza (*Yr7*) and Lemhi (*Yr5*)

mutants are available through the JIC Germplasm Resource Unit (www.seedstor.ac.uk).

Competing interests

A patent application based on this work has been filed (United Kingdom Patent Application

No. 1805865.1).

25

668 **Figure legends**

669 **Figure 1**: *Yr5* **and** *YrSP* **are allelic, but paralogous to** *Yr7***.**

670 **a**, Left: Wild-type and selected EMS-derived susceptible mutant lines for *Yr7*, *Yr5*, and *YrSP*

671 (Supplementary Table 3 and 3) inoculated with *Pst* isolate 08/21 (*Yr7*), *Pst* 150 E16 A+

672 (*Yr5*), or *Pst* 134 E16 A+ (*YrSP*). Right: Candidate gene structures, with mutations in red,

673 and their predicted effects on the translated protein. **b**, Schematic representation of the

674 physical interval of the *Yr* loci. The *Yr7/Yr5/YrSP* locus is shown in orange on chromomsome

675 2B with previously published SSR markers in black. Markers developed in this study to

676 confirm the genetic linkage between the phenotype and the candidate contigs are shown as

677 black lines underneath the chromosme. *Yr* loci mapping intervals are defined by the red

678 horizontal lines. A more detailed genetic map is shown in Supplementary Figure 3.

679

680 **Figure 2:** *Yr7* **and** *Yr5/YrSP* **encode integrated BED-domain immune receptor genes.**

681 **a**, Schematic representation of the Yr7, Yr5, and YrSP protein domain organisation. BED

682 domains are highlighted in red, NB-ARC domains are in blue, LRR motifs from NLR-

683 Annotator are in dark green, and manually annotated LRR motifs (xxLxLxx) are in light

684 green. Black triangles represent the EMS-induced mutations within the protein sequence. The

685 plot shows the degree of amino acid conservation (50 amino acid rolling average) between

686 Yr7 and Yr5 proteins, based on the conservation diagram produced by Jalview (2.10.1) from

687 the protein alignment. Regions that correspond to the conserved domains have matching

688 colours. The amino acid changes between Yr5 and YrSP are annotated in black on the YrSP

689 protein. **b**, Five Yr5/YrSP haplotypes were identified in this study. Polymorphisms are

690 highlighted across the protein sequence with orange vertical bars for polymorphisms shared

691 by at least two haplotypes and blue vertical bars for polymorphisms that are unique to the

27

692   corresponding haplotype. Matching colours across protein structures illustrate 100%

693   sequence conservation.

694   **Figure 3: BED domains from BED-NLRs and non-NLR proteins are distinct.**

695   **a**, Numbers of NLRs in the syntenic regions across grass genomes (see Supplementary Figure

696   7), including BED-NLRs. **b**, WebLogo (http://weblogo.berkeley.edu/logo.cgi) diagram

697   showing that the BED-I and BED-II domains are distinct, with only the highly conserved

698   residues that define the BED domain (red bars) being conserved between the two types. **c**,

699   Gene structure most commonly observed for BED-NLRs and BED-BED-NLRs within the

700   *Yr7*/*Yr5*/*YrSP* syntenic interval. **d**, Neighbour-net analysis based on uncorrected *P* distances

701   obtained from alignment of 153 BED domains including the 108 BED-containing proteins

702   (including 25 NLRs) from RefSeq v1.0, BED domains from NLRs located in the syntenic

703   region as defined in Supplementary Figure 7, and BED domains from Xa1 and ZBED from

704   rice. BED-I and II clades are highlighted in purple and blue, respectively. BED domains from

705   the syntenic regions not related to either of these types are in red. BED domains derived from

706   non-NLR proteins are in black and BED domains from BED-NLRs outside the syntenic

707   region are in grey. Seven BED domains from non-NLR proteins were close to BED domains

708   from BED-NLRs. Supplementary Figure 9 includes individual labels.

28

709 **Supplementary Figure 1: Deployment of *Yr7* cultivars in the field is correlated with an**

710 **increase in the prevalence of *Pst* isolates virulent on *Yr7* in the UK.**

711 Percentage of total harvested weight of wheat cultivar carrying *Yr7* (green) and the

712 proportion of *Pst* isolates that are virulent to Yr7 (orange) from 1990 to 2016 in the United

713 Kingdom. See Supplementary Table 2 for a summary of the data.

714

715 **Supplementary Figure 2: Identification of candidate contigs for the *Yr* loci using**

716 **MutRenSeq.**

717 View of RenSeq reads from the wild-type and EMS-derived mutants mapped to the best

718 candidate contigs identified with MutantHunter for the three genes targeted in this study.

719 From top to bottom: vertical black lines represent the *Yr* loci, coloured rectangles depict the

720 motifs identified by NLR-Annotator (each motif is specific to a conserved NLR domain[56]),

721 while read coverage (grey histograms) is indicated on the left, e.g. [0 - 149], and the line from

722 which the reads are derived on the right, e.g. CadWT for Cadenza wild-type. Vertical bars

723 represent the position of the SNPs identified between the reads and reference assembly – red

724 shows C to T transitions and green G to A transitions. Black boxes highlight SNP for which

725 the coverage was relatively low, but still higher than the 20x detection threshold. The top

726 view shows the *Yr7* allele annotated from the Cadenza genome assembly before manual

727 curation (Supplementary File 3). Vertical black lines illustrate the assembled candidate

728 contigs and the one that was formerly *de novo* assembled from Cadenza RenSeq data, lacking

729 the 5' region containing the BED domain and thus the Cad903 mutation. The middle view

730 illustrates the *Yr5* locus annotated from the Lemhi-*Yr5 de novo* assembly. The results are

731 similar to those described above for *Yr7*. The full locus was *de novo* assembled. The bottom

732 view illustrates the *YrSP* locus annotated from the AvocetS-YrSP *de novo* assembly with the

733 four identified susceptible mutants all carrying a mutation in the candidate contig. The full

734 locus was *de novo* assembled.

735

736 **Supplementary Figure 3: Candidate contigs identified by MutRenSeq are genetically**

737 **linked to the *Yr* loci mapping interval.**

738 Schematic representation of chromosome 2B from Chinese Spring (RefSeq v1.0) with the

739 positions of published markers linked to the *Yr* loci and surrounding closely linked markers

740 that were used to define their physical position (orange rectangle). The chromosome is

741 depicted as a close-up of the physical locus indicating the positions of KASP markers that

742 were used for genetic mapping (horizontal bars, Supplementary Table 15). Blue colour refers

29

743   to *Yr7*, red to *Yr5*, and purple to *YrSP*. The black arrow points to the NLR cluster containing

744   the best BLAST hits for *Yr7* and *Yr5*/*YrSP* on RefSeq v1.0. Coloured lines link the physical

745   map to the corresponding genetic map for each targeted gene (see Methods). Genetic

746   distances are expressed in centiMorgans (cM).

747

748   **Supplementary Figure 4**: **Yr7, Yr5 and YrSP proteins do not encode for a Coiled-Coil**

749   **domain in the N-terminus.**

750   Graphical outputs from the COILS prediction programm in three sliding windows (14, 21,

751   and 28 amino acid, shown in green, blue, and red, respectively) for Yr5 and Yr7 with or

752   without the BED domain (left) and characterised canonical NLRs: Sr33[21], Mla10[20], Pm3[22]

753   and RPS5[57]. The X axis shows the amino acid positions and the Y axis the probability of a

754   coiled coil domain formation. There was no difference in the prediction between the two Yr

755   proteins with or without their BED domain. The 14 amino acid sliding window is the least

756   accurate according to the user manual, consistent with the additional peaks observed in Sr33,

757   Mla10 and Pm3 that were not annotated as CC domains in the corresponding publications[20–

758   22]. Thus, the peak at position 1,200 in Yr5 is unlikely to represent a CC domain. We

759   performed a BLASTP search with the N-terminal region of the Yr5 and Yr7 proteins (from

760   Met to the first amino-acid encoding the NB-ARC) with or without the BED domain and the

761   best hits were proteins predicted to encode BED-NLRs from *Aegilops tauschii*, *Triticum*

762   *uratu* and *Oryza Sativa* (data not shown). Based on the COILS prediction and the BLAST

763   search, we concluded that Yr7 and Yr5/YrSP do not encode CC domains.

764

765   **Supplementary Figure 5: Pedigrees of selected Thatcher-derived cultivars and their *Yr7***

766   **allelic status.**

767   Pedigree tree of Thatcher-derived cultivars where each circle represents a cultivar and the

768   size of the circle is proportional to its prevalence in the tree. Colours illustrate the genotype

769   with red showing the absence of *Yr7* and yellow its presence. Cultivars in grey were not

770   tested or are intermediate crosses. *Yr7* originated from *Triticum durum* cv. Iumillo and was

771   introgressed into hexaploid wheat through Thatcher (indicated by arrow). Each *Yr7* positive

772   cultivar is related to a parent that was also positive for *Yr7*. Figure was generated using the

773   Helium software[45] (v1.17).

774

775   **Supplementary Figure 6: Diagnostic genetic marker for *Yr5*.**

776

30

777   The *Yr5*-specific insertion was used to generate a PCR amplification product of 1,281 bp for

778   *Yr5* or a shorter amplicon for the absence of the insertion in *YrSP*, Claire, and Paragon (507

779   bp). *Yr5* positive lines include the *Yr5* spelt donor and *Yr5* near-isogenic lines AvocetS-*Yr5*

780   and Lemhi-*Yr5*. *YrSP* donor Spaldings Prolific and *YrSP* near-isogenic lines AvocetS-*YrSP*

781   carry the shorter alternate allele, similar to the Claire, Cadenza and Paragon alleles identified

782   in Figure 2. Negative controls include AvocetS and H_2O. Size marker is shown on the left.

783

784   **Supplementary Figure 7: Expansion of BED-NLRs in the Triticeae and presence of**

785   **conserved BED-BED-NLRs aross the syntenic region.**

786   Schematic representation of the physical loci containing *Yr7* and *Yr5*/*YrSP* homologs on

787   RefSeq v1.0 and its syntenic regions. The syntenic region is flanked by conserved non-NLR

788   genes (orange arrows). Black arrows represent canonical NLRs and purple/blue/red arrows

789   represent different types of BED-NLRs based on their BED domain and their relationship

790   identified in Figure 3 and Supplementary Figure 8. Black lines represent phylogenetically

791   related single NLRs located between the two NLR clusters illustrated in Supplementary

792   Figure 9. Details of genes are reported in Supplementary File 4.

793

794   **Supplementary Figure 8: The *Yr* loci are phylogenetically related to nearby NLRs on**

795   **RefSeq v1.0 and their orthologs.**

796   Phylogenetic tree based on translated NB-ARC domains from NLR-Annotator. Node labels

797   represent bootstrap values for 1,000 replicates. The tree was rooted at mid-point and

798   visualized with Dendroscope v3.5.9. The colour pattern matches that of Figure 3 to highlight

799   BED-NLRs with different BED domains.

800

801   **Supplementary Figure 9: Neighbour-net analysis network as shown in Figure 3 with**

802   **identifiers.**

803   Neighbour-net analysis based on uncorrected *P* distances obtained from alignment of 153

804   BED domains including the 108 BED-containing proteins (including 25 NLRs) from RefSeq

805   v1.0, BED domains from NLRs located in the syntenic region as defined in Supplementary

806   Figure 7, and BED domains from Xa1 and ZBED from rice. BED-I and II clades are

807   highlighted in purple and blue, respectively. BED domains from the syntenic regions not

808   related to either of these types are in red. BED domains derived from non-NLR proteins are

809   in black and BED domains from BED-NLRs outside the syntenic region are in grey. Seven

810   BED domains from non-NLR proteins were close to BED domains from BED-NLRs.

811

Supplementary Figure 10: BED-NLRs and BED-containing proteins are not differentially expressed in yellow rust-infected susceptible and resistant cultivars.

Heatmap representing the normalised read counts (Transcript Per Million, TPM) from the reanalysis of published RNAseq data[29] for all the BED-containing proteins, BED-NLRs and canonical NLRs located in the syntenic region annotated on RefSeq v1.0. Lack of expression is shown in white and expression levels increase from blue to red. Asterisks show cases where several gene models were overlapping with NLR loci identified with NLR Annotator. The colour pattern matches that of Figure 3 to highlight BED-NLRs with different BED domains. Orange labels show the expression of the canonical NLRs located within the syntenic interval. The seven non-NLR BED genes whose BED domain clustered with the ones from BED-NLR proteins in Figure 3 and Supplementary Figure 9 are indicated by black triangles.

824

Supplementary Table 1: Summary of *Pst* isolates tested on *Yr5* differential lines from 2004 to 2017 in different regions.

Overall, >6,000 isolates from 44 countries displaying >200 different pathotypes were tested on *Yr5* materials and no virulence was recorded apart from one isolate from Australia, PST 360 E137 A+[14]. Data were obtained from public databases and reports on yellow rust surveillance, whose references are recorded. It is important to note that we report here the number of identified pathotypes for a given region and database. Similar pathotypes could thus have been counted twice if identified in different regions.

833

Supplementary Table 2: Harvested weight of known *Yr7* cultivarsfrom 1990 to 2016 and *virYr7* prevalence among UK *Pst* isolates.

Proportion of harvested *Yr7* wheat cultivars in the UK from 1990 to 2016. The prevalence of yellow rust isolates virulent to *Yr7* across this time period is shown in the top row. Original data from NIAB-TAG Seedstats journal (NIAB-TAG Network) and the UK Cereal Pathogen Virulence Survey (http://www.niab.com/pages/id/316/UKCPVS).

840

Supplementary Table 3: Plant materials analysed for the present study with the different *Pst* isolates used for the pathology assays.

843

32

844 **Supplementary Table 4: Plant material submitted for Resistance gene enrichment**
845 **Sequencing (RenSeq).**
846 From left to right: Mutant line identifier, targeted gene, score when infected with *Pst*
847 according to the Grassner and Straib scale, mutation position, coverage of the mutation (at
848 least 99% of the reads supported the mutant base in the mutant reads), predicted effect of the
849 mutation on the protein sequence, comments. Lines with the same mutations are highlighted
850 with matching colours.
851

852 **Supplementary Table 5: Genome assemblies used in the present study.**
853 Summary of the available genome assemblies[58,59] that were used for the *in silico* allele
854 mining and synteny analysis across rice, *Brachypodium*, barley and different Triticeae
855 accessions.
856

857 **Supplementary Table 6: *In silico* allele mining for *Yr7* and *Yr5/YrSP* in available**
858 **genome assemblies for wheat.**
859 Table presents the percentage identity (% ID) of the identified alleles and matching colours
860 illustrate identical haplotypes. Investigated genome assemblies are shown in Supplementary
861 Table 5.
862

863 **Supplementary Table 7: Polymorphisms between Yr5 protein and its identified alleles**.
864 Positions of the polymorphic amino acids across the five Yr5/YrSP proteins. Polymorphisms
865 falling into the BED and NB-ARC domains are shown in red and blue, respectively.
866

867 **Supplementary Table 8: Presence/absence of *Yr7* alleles in a selected panel of Cadenza-**
868 **derivatives and associated responses to different *Pst* isolates (avirulent to *Yr7*: *Pst***
869 **15/151 and 08/21; virulent to *Yr7*: 14/106).**
870 Infection types were grouped into two categories: 1 for resistant and 2 for susceptible. We
871 used Vuka as a positive control for inoculation and absence of *Yr7*. The typical response of a
872 *Yr7* carrier would thus be 1 – 1 – 2, although some cultivars might carry other resistance
873 genes that can lead to a 1 – 1 – 1 profile (e.g. Cadenza). Cultivars that were positive for *Yr7*
874 had either one or the other profile so none of them was susceptible to a *Pst* isolate that is
875 avirulent to *Yr7*. Few cultivars (e.g Bennington, KWS-Kerrin, Brando) were susceptible to
876 one of the two isolates avirulent to *Yr7* in addition to their susceptibility to the *Yr7*-virulent
877 isolate. However, none of them carried the *Yr7* allele.

878

879 **Supplementary Table 9: Presence/absence of *Yr7* and *YrSP* in different wheat**

880 **collections.** We used Vuka, AvocetS and Solstice as negative controls for the presence of *Yr7*

881 and *YrSP* and AvocetS-*Yr* near-isogenic lines as controls for the corresponding *Yr* gene. We

882 genotypied different collections: (i) a set of potential *Yr7* carriers based on literature research,

883 (ii) a set of cultivars that belonged to the UK AHDB Recommended List

884 (https://cereals.ahdb.org.uk/varieties/ahdb-recommended-lists.aspx) between 2005 and 2018

885 (labelled 2005-2018-UK_RL), (iii) the Gediflux collection that includes modern European

886 bread wheat cultivars (1920-2010)[25], (iv) a core set of the Watkins collection, which

887 represent a set of global bread wheat landraces collected in the 1920-30s[24]. Most of the

888 putative *Yr7* carriers were positive for all the *Yr7* markers apart from Aztec, Chablis and

889 Cranbrook. Chablis was susceptible to the *Pst* isolates that were avirulent to *Yr7* so it

890 probably does not carry the gene. Regarding the 2005-2018-UK_RL results were consistent

891 across already tested cultivars: Cadenza, Cordiale, Cubanita, Grafton and Skyfall were

892 already positive in Supplementary Table 8. Energise, Freiston, Gallant, Oakley and

893 Revelation were negative on both panels as well. Results were thus consistent across different

894 sources of DNA. *Yr7*-containing cultivars are not prevalent in the 2005-2018 Recommended

895 List set, however, this gene is present in Skyfall, which is currently one of the most harvested

896 cultivars in the UK (Supplementary Table 2). We tested the *YrSP* marker on this set and it

897 was positive only for AvocetS-*YrSP*. The frequency of *Yr7* was relatively low in the Gediflux

898 panel (4%). This is consistent with results in Supplementary Table 2: *Yr7* deployment started

899 in the UK in 1992 with Cadenza and it was rarely used prior to that date. The same was

900 observed in the subset of the Watkins collection (10%) where landraces that were positive for

901 *Yr7* all originated from India and the Mediterranean basin. *Yr7* was introgressed into

902 Thatcher (released in 1936) from Iumillo, which originated from Spain and North-Africa

903 (Genetic Resources Information System for Wheat and Tritical -

904 http://www.wheatpedigree.net/). Iumillo is likely to be pre-1920s and these landraces are all

905 bread wheats so they might have inherited it from another source. However, there is no

906 evidence for *Yr7* coming from another source than Iumillo in the modern bread wheat

907 cultivars.

908

909 **Supplementary Table 10**: **Presence/absence of *Yr5* alleles in selected cultivars.**

910 A subset of the aforementioned collection was investigated for the *Yr5* presence. "Yes" in the

911 *Yr5* column refers to amplification of the 1,281 bp amplicon with the *Yr5*-Insertion primers

912 (Supplementary Figure 6). "Yes" in the *Yr5* alternate alleles column refers to the

913 amplification of the 507 bp amplicon that was identified for AvocetS-*YrSP*, Claire, Cadenza

914 and Paragon in Supplementary Figure 6. "Yes" in the no amplification column refers to

915 identification of a profile similar to the one found for AvocetS in Supplementary Figure 6.

916

917 **Supplementary Table 11: Identified BED-containing proteins in RefSeq v1.0 based on a**

918 **hmmer scan analysis (see Methods).**

919 Several features are added: number of identified BED domains and the presence of other

920 conserved domains present, the best BLAST hit from the non-redundant database of NCBI

921 with its description and score, and whether the BED domain was related to BED domains

922 from NLR proteins based on the neighbour network shown in Supplementary Figure 8.

923

924 **Supplementary Table 12: Transcripts per Million-normalised read counts from the re-**

925 **analysis of published RNA-Seq data[29] and associated differential expression analysis**

926 **performed with DESeq2.**

927

928 **Supplementary Table 13: Sequencing details of RenSeq data generated in this study.**

929

930 **Supplementary Table 14: *De novo* assemblies generated from the corresponding**

931 **RenSeq data.**

932

933 **Supplementary Table 15: Primers designed to map and clone *Yr7*, *Yr5*, and *YrSP*.**

934 Note that KASP assays require the addition of the corresponding 5' -tails for the two KASP

935 primers

936

937 **Supplementary Table 16: Diagnostic markers for *Yr7*, *Yr5*, and *YrSP*.**

938 Note that KASP assays require the addition of the corresponding 5' -tails for the two KASP

939 primers.

940

941 **Supplementary Table 17: Passport data of tested *T. dicoccoides* accessions**

942

943 **Supplementary File 1: Annotation of the *Yr7* locus in Cadenza with exon/intron**

944 **structure, positions of mutations and the position of primers for long-range PCR and**

945 **nested PCRs that were carried out prior to Sanger sequencing (Supplementary Table**

946 **15)**. The file also includes the derived CDS and protein sequences with annotated conserved

947 domains. Amino acids encoding the BED domain are shown in red and those encoding the

948 NB-ARC domain are in blue. LRR repeats identified with NLR Annotator are highlighted in

949 dark green and manually annotated LRR motifs xxLxLxx are underlined and in bold black.

950

951 **Supplementary File 2**: **Annotation of the *Yr5/YrSP* locus in Lemhi-*Yr5* and AvocetS-**

952 ***YrSP*, respectively, with exon/intron structure, the position of mutations and the**

953 **position of primers for long-range PCR and nested PCRs that were carried out prior to**

954 **Sanger sequencing (Supplementary Table 15)**. The derived CDS and protein sequences

955 with annotated conserved domains are also shown. Amino acids encoding the BED domain

956 are shown in red and those encoding the NB-ARC domain are in blue. LRR repeats identified

957 with NLR Annotator are highlighted in dark green and manually annotated LRR motifs

958 xxLxLxx are underlined and in bold black. Design of the *Yr5* PCR marker is shown at the

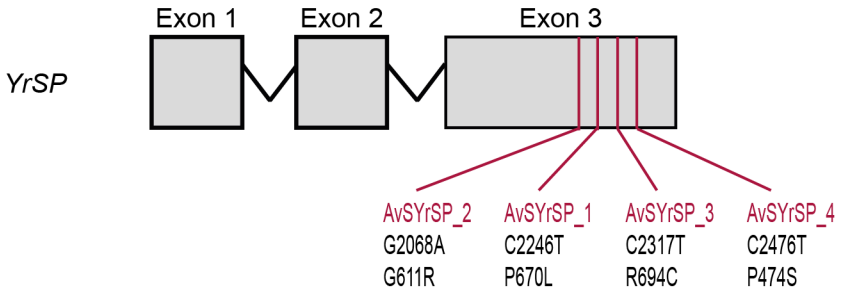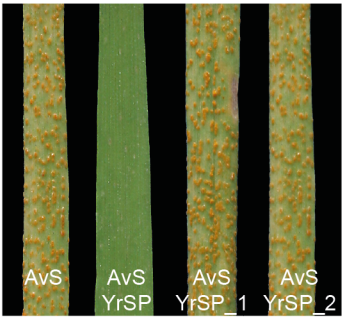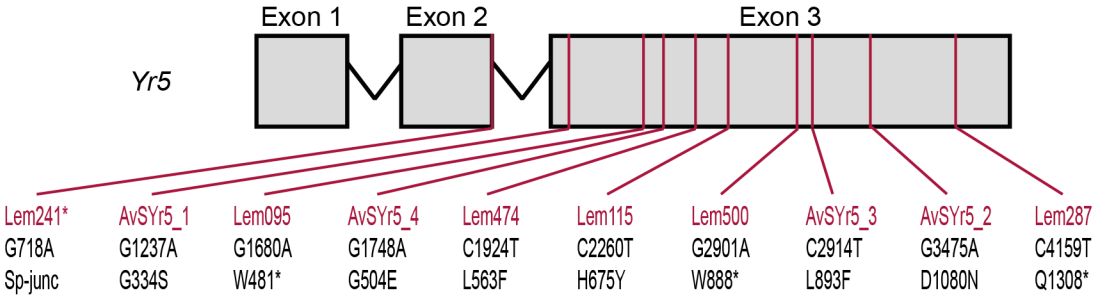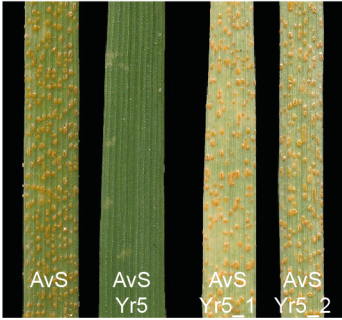959 end of the file with the insertion that is specific to *Yr5* when compared to *YrSP* and Claire.
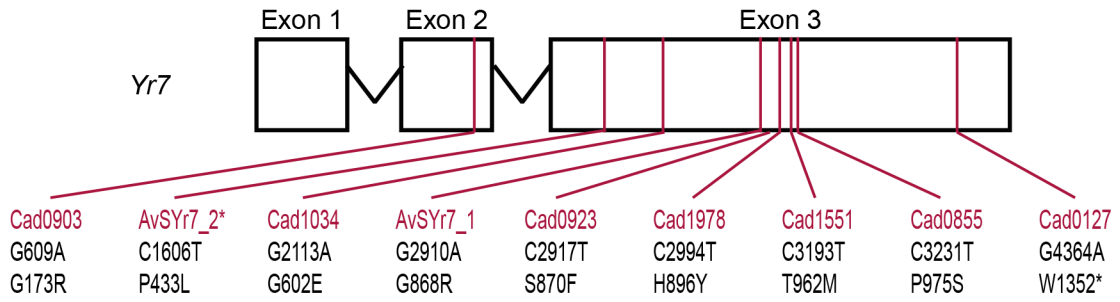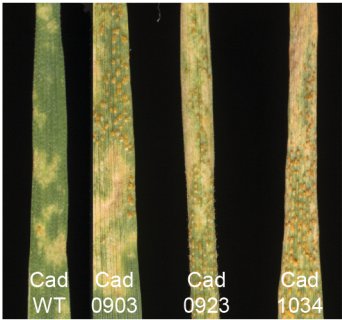
960

961 **Supplementary File 3**: **Curation of the *Yr7* locus in the Cadenza genome assembly based**

962 **on Sanger sequencing results.**

963 Comments show the position of the unknown bases ("N") in the "Yr7_with_Ns" sequence.

964 Curation based on Sanger sequencing data is shown in bold black in the "curated_Yr7"

965 sequence with the 39 bp insertion and 129 bp deletion. Allele mining for *Yr7* in the Paragon

966 assembly showed that a similar assembly issue might have occurred for this cultivar (same

967 annotation in the "Yr7_Paragon_with_Ns" sequence). This is consistent with the fact that

968 both assemblies were produced with the same pipeline (Supplementary Table 5). We used

969 RenSeq data available for Paragon and performed an alignment as described for the

970 MutRenSeq pipeline against Cadenza NLRs with the curated *Yr7* loci included. A screen

971 capture of the mapping is shown. Only one SNP was identified (75% Cadenza, 25%

972 Paragon). Across the six reads supporting the alternate base, four displayed several SNPs and

973 mapped to an additional Cadenza NLR. This provides evidence for the presence of the

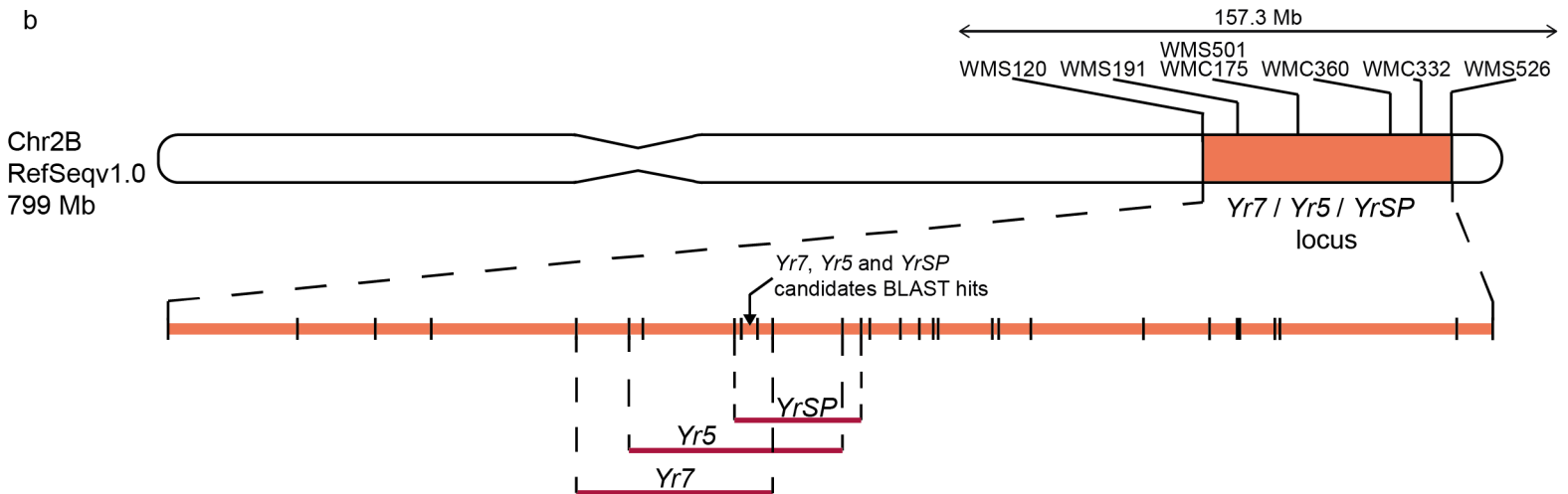974 identical gene in Paragon which is supported by phenotypic data.

975

976 **Supplementary File 4**: **Syntenic region across different grasses (Supplementary Table 5)**

977 **and the NLR loci identified with NLR-Annotator**. See Methods for a detailed explanation

978 of the analysis and Supplementary Figure 7 for an illustration.

979

36

980   **Supplementary File 5**: **Curated sequences of BED-NLRs from chromosome 2B and**

981   **Ta_2D7**. Exons are highlighted with different colours (yellow, green, blue, pink). Amino

982   acids encoding the BED domain are shown in red and those encoding the NB-ARC domain

983   are in blue. LRR repeats identified with NLR Annotator are highlighted in dark green and

984   manually annotated LRR motifs xxLxLxx are underlined and in bold black.

a

Yr7
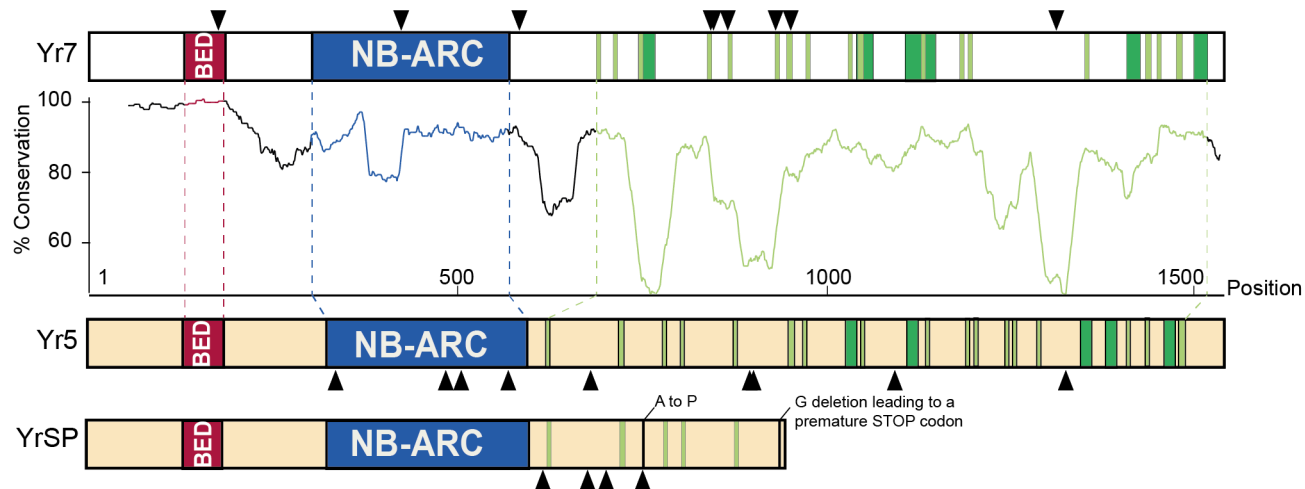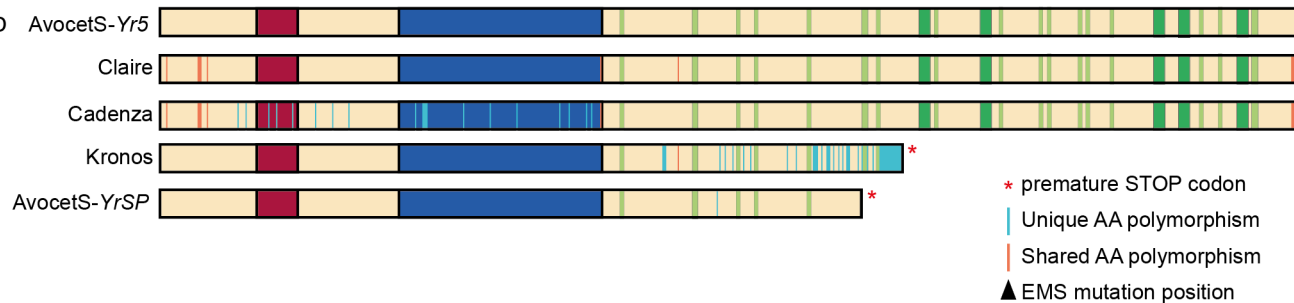
% Conservation

Yr5

YrSP

A to P

G deletion leading to a
premature STOP codon

b

AvocetS-*Yr5*

Claire

Cadenza

Kronos

AvocetS-*YrSP*

* premature STOP codon

| Unique AA polymorphism

| Shared AA polymorphism

▲ EMS mutation position

a

Syntenic interval	#NLRs	#BED NLRs	#BED NLRs-I	#BED NLRs-II	#BED NLRs-I-II
Rice	6	2	-	-	-
Brachypodium	4	4	1	1	-
Barley	2	-	-	-	-
Aegilops tauschii (D)	8	4	1	1	1
Hexaploid wheat (D)	6	2	1	-	1
Tetraploid wheat (A)	8	1	1	-	-
Hexaploid wheat (A)	12	5	3	2	-
Tetraploid wheat (B)	20	10	6	2	1
Hexaploid wheat (B)	13	5	1	1	3

b

BED-I

BED-II

c

Exon 1 Exon 2 Exon 3
BED NB-ARC LRRs

Exon 1 Exon 2 Exon 3 Exon 4
BED I BED II NB-ARC LRRs

d

Legend
— non-NLR BED-containing proteins
— wheat BED-NLRs outside synteny
— BED-NLRs within synteny
— BED-I
— BED-II

BED-I related
Yr5
YrSP *Yr7*
Xa1
BED-II related

0.1